

Universal thermodynamic topological classes of rotating black holes

Xiao-Dan Zhu¹, Wentao Liu², and Di Wu^{1*}

¹*School of Physics and Astronomy, China West Normal University,
Nanchong, Sichuan 637002, People's Republic of China*

²*Department of Physics, Key Laboratory of Low Dimensional Quantum Structures and Quantum Control of Ministry of Education,
and Synergetic Innovation Center for Quantum Effects and Applications,
Human Normal University, Changsha, Hunan 410081, People's Republic of China*

(Dated: November 28, 2024)

In a recent study, Wei *et al.* [*Phys. Rev. D* **110**, L081501 (2024)] proposed a universal classification scheme that interprets black hole solutions, including the four-dimensional Schwarzschild, Reissner-Nordström (RN), Schwarzschild-AdS, and RN-AdS black hole solutions, as topological defects within the thermodynamic parameter space, and then divides black hole solutions into four distinct classes, denoted as W^{1-} , W^{0+} , W^{0-} , and W^{1+} , offering insights into deeper aspects of black hole thermodynamics and gravity. In this paper, we investigate the universal thermodynamic topological classification of the singly rotating Kerr black holes in all dimensions, as well as the four-dimensional Kerr-Newman black hole. We show that the innermost small black hole states of the $d \geq 6$ singly rotating Kerr black holes are thermodynamically unstable, while those of the four-dimensional Kerr-Newman black hole and the $d = 4, 5$ singly rotating Kerr black holes are thermodynamically stable. On the other hand, the outermost large black holes exhibit unstable behavior in all these cases. At the low-temperature limit, the $d \geq 6$ singly rotating Kerr black holes have one large thermodynamically unstable black hole state, while the four-dimensional Kerr-Newman black hole and the $d = 4, 5$ singly rotating Kerr black holes feature one large unstable branch and one small stable branch. Conversely, at the high-temperature limit, the $d \geq 6$ singly rotating Kerr black holes exhibit a small unstable black hole state, while the four-dimensional Kerr-Newman black hole and the $d = 4, 5$ singly rotating Kerr black holes have no black hole states at all. Consequently, we demonstrate that the $d \geq 6$ singly rotating Kerr black holes belong to the class W^{1-} , whereas the four-dimensional Kerr-Newman and $d = 4, 5$ singly rotating Kerr black holes belong to the class W^{0+} , thereby further support the conjecture proposed in [*Phys. Rev. D* **110**, L081501 (2024)].

I. INTRODUCTION

Black holes, among the most extraordinary and captivating objects in the universe, have long been the focus of intensive theoretical and observational research. On the observational side, recent breakthroughs include direct imaging of black hole shadows [1–5] by the Event Horizon Telescope (EHT) [6, 7] and the detection of gravitational waves resulting from black hole mergers [8, 9]. On the theoretical side, recent advances in understanding the topology of black holes have provided novel insights into the nature of gravity, with significant contributions from studies on light rings [10–19], timelike circular orbits [20–22], thermodynamic phase transitions [23–50], and special thermodynamic topological classifications [51–62].¹

Quite recently, in Ref. [96], Wei *et al.* further developed the method initially proposed in Ref. [51] by using the generalized off-shell free energy to treat black hole solutions as topological thermodynamic defects. They analyzed the asymptotic behaviors of the constructed vector and, using four-dimensional Schwarzschild, Reissner-Nordström (RN), Schwarzschild-AdS, and RN-AdS black holes as examples, categorized black hole solutions into four distinct topological classes: W^{1-} , W^{0+} , W^{0-} , W^{1+} .² This classification of-

fers new insights into the fundamental nature of black hole thermodynamics and gravity. A brief introduction of this approach is presented below.

According to Ref. [96], one can first introduce the generalized off-shell Helmholtz free energy as [97]

$$\mathcal{F} = M - \frac{S}{\tau}, \quad (1)$$

where M and S represent the mass and entropy of the black hole, respectively, and the additional variable τ can be interpreted as the inverse temperature of the cavity enclosing the black hole. The generalized Helmholtz free energy exhibits only on-shell properties and reduces to the standard Helmholtz free energy $F = M - TS$ [98, 99] of the black hole when $\tau = \beta = T^{-1}$. By including an additional parameter $\Theta \in (0, \pi)$, one can define a two-dimensional vector ϕ based on the gradient of $\hat{\mathcal{F}} = \mathcal{F} + 1/\sin\Theta$, given by

$$\phi = \left(\frac{\partial \hat{\mathcal{F}}}{\partial r_h}, \frac{\partial \hat{\mathcal{F}}}{\partial \Theta} \right), \quad (2)$$

where r_h is the event horizon radius of the black hole. A thorough analysis demonstrates that the black hole states precisely align with the zero points of the vector ϕ . Then, by applying Duan's ϕ -mapping topological current theory [100–102], a topological invariant, also referred to as the winding number w , can be attributed to each zero point or black hole state [51]. Utilizing the above framework, the heat capacity of a black hole state can be either positive or negative, corresponding to winding numbers of $w = +1$ and $w = -1$, respectively. Here, a positive winding number indicates a locally stable black hole

* Corresponding author: wdcwnu@163.com

¹ The black hole solutions are classified into three categories based on different topological numbers. Please see more examples in Refs. [63–95] for the latest developments.

² For the details of the four topological classes, please see Appendix A.

state, while a negative winding number signifies a locally unstable state. The topological number W , defined as

$$W = \sum_{i=1}^N w_i, \quad (3)$$

is obtained by summing all the winding numbers w_i associated with the i th zero point of the field ϕ , where N is the total number of zero points. This topological number W serves as a classification parameter for black hole systems, thereby providing a novel way to classify different black hole solutions. It is important to highlight that the local winding number w_i serves as an effective tool for characterizing local thermodynamic stability. Thermodynamically stable black holes correspond to positive w_i values, while unstable black holes correspond to negative values. Conversely, the global topological number W reflects the difference between the quantities of stable and unstable black holes within a classical solution at a fixed temperature. Thus, the local winding number differentiates between stable and unstable phases of black holes at a given temperature and aids in classifying black hole solutions based on the global topological number. Furthermore, black holes within the same universal thermodynamic topological class exhibit similar thermodynamic properties, regardless of their geometric classification. This finding not only highlights the intrinsic connections between different black hole solutions but also provides a new perspective for studying the thermodynamic phase transitions and stability of black holes. Through this classification, we can better understand the mechanisms behind black hole behavior and their impact on thermodynamic stability and phase transitions. Since astronomical observations have largely focused on rotating black holes, exploring their universal thermodynamic topological classes is both essential and necessary. This provides the main motivation for this paper.

In this paper, we investigate the universal thermodynamic topological classification of the singly rotating Kerr black holes in arbitrary dimensions, and the four-dimensional Kerr-Newman black hole. We find that the $d \geq 6$ singly rotating Kerr black holes belong to the class W^{1-} , while the four-dimensional Kerr-Newman and $d = 4, 5$ singly rotating Kerr black holes belong to the class W^{0+} . Compared to our previous work [52], we provide new insights into the thermodynamic stability of the innermost small black hole state and the outermost large black hole state, as well as their thermodynamic properties in both the low-temperature and high-temperature limits. Understanding these aspects is crucial for revealing the complex behavior of rotating black holes, as it helps elucidate their phase transitions and stability conditions. Furthermore, we explore the systematic orderings of the black hole states corresponding to increasing horizon radius, which sheds light on the underlying mechanisms governing black hole thermodynamics. The remaining part of this paper is organized as follows. In Sec. II, we explore the universal thermodynamic topological class of the four-dimensional Kerr black hole and analyze its state systematic ordering and universal thermodynamic behavior. In Secs. III and IV, this analysis is extended to d -dimensional singly rotating Kerr black

holes and the four-dimensional Kerr-Newman black hole, respectively. Sec. V provides a summary of our findings and outlooks for future work.

II. FOUR-DIMENSIONAL KERR BLACK HOLE

In this section, we will focus on the universal thermodynamic topological class of the four-dimensional Kerr black hole, whose metric in the asymptotically nonrotating frame has the form [103]

$$ds^2 = -\frac{\Delta_r}{\Sigma} (dt - a \sin^2 \theta d\varphi)^2 + \frac{\Sigma}{\Delta_r} dr^2 + \Sigma d\theta^2 + \frac{\sin^2 \theta}{\Sigma} [adt - (r^2 + a^2)d\varphi]^2 \quad (4)$$

where

$$\Delta_r = r^2 + a^2 - 2mr, \quad \Sigma = r^2 + a^2 \cos^2 \theta,$$

in which m and a are the mass and the rotation parameters of the black hole.

The thermodynamic quantities of the four-dimensional Kerr black hole can be derived using standard techniques, yielding the following elegant expressions [104, 105]:

$$M = m, \quad J = ma, \quad \Omega = \frac{a}{r_h^2 + a^2}, \quad (5)$$

$$S = \pi(r_h^2 + a^2), \quad T = \frac{r_h^2 - a^2}{4\pi r_h(r_h^2 + a^2)},$$

where the event horizon is located at $r_h = m + \sqrt{m^2 - a^2}$. It is easy to find that the Hawking temperature of the four-dimensional Kerr black hole approaches zero both in the limit $r \rightarrow \infty$ and in the extremal case, where $r \rightarrow r_m = m = a$, with r_m being the minimal horizon radius of the four-dimensional Kerr black hole. Consequently, the inverse temperature $\beta(r_h)$ exhibits

$$\beta(r_m) = \infty, \quad \beta(\infty) = \infty \quad (6)$$

at these asymptotic limits. The defect curve $\beta(r_h)$ must remain analytic over the range (r_m, ∞) .

Using the definition of the generalized off-shell Helmholtz free energy (1), one can easily obtain

$$\mathcal{F} = \frac{r_h^2 + a^2}{2r_h} - \frac{\pi(r_h^2 + a^2)}{\tau} \quad (7)$$

for the four-dimensional Kerr black hole. Thus,

$$\hat{\mathcal{F}} = \mathcal{F} + \frac{1}{\sin \Theta} = \frac{r_h^2 + a^2}{2r_h} - \frac{\pi(r_h^2 + a^2)}{\tau} + \frac{1}{\sin \Theta}. \quad (8)$$

From Eq. (2), the components of the vector ϕ can be computed as

$$\phi^{r_h} = \frac{1}{2} - \frac{a^2}{2r_h^2} - \frac{2\pi r_h}{\tau}, \quad (9)$$

$$\phi^\Theta = -\cot \Theta \csc \Theta. \quad (10)$$

TABLE I. The direction indicated by the arrows of ϕ^{r_h} and the corresponding topological number for the four-dimensional Kerr black hole.

Black hole solutions	I_1	I_2	I_3	I_4	W
$d = 4$ Kerr black hole	\leftarrow	\uparrow	\leftarrow	\downarrow	0

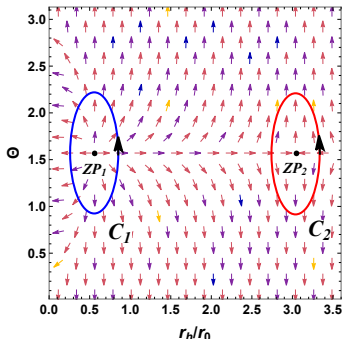


FIG. 1. The arrows represent the unit vector field on a portion of the $r_h - \Theta$ plane for the four-dimensional Kerr black hole with $\beta/r_0 = 40$ and $a/r_0 = 0.5$. The zero points (ZPs) marked with black dots are at $(r_h/r_0, \Theta) = (0.55, \pi/2)$, and $(3.10, \pi/2)$, for ZP_1 , and ZP_2 , respectively. The blue contours C_i are closed loops surrounding the zero points.

Therefore, the defect curve, which represents the set of the zero points of the vector in the parameter space, can be readily obtained by solving Eq. (9).

We now examine the asymptotic behavior of the vector ϕ at the boundary corresponding to Eq. (6). This boundary can be described by the contour $C = I_1 \cup I_2 \cup I_3 \cup I_4$, where $I_1 = \{r_h = \infty, \Theta \in (0, \pi)\}$, $I_2 = \{r_h \in (\infty, r_m), \Theta = \pi\}$, $I_3 = \{r_h = r_m, \Theta \in (\pi, 0)\}$, and $I_4 = \{r_h \in (r_m, \infty), \Theta = 0\}$. This contour covers all relevant parameter regions. The setup of ϕ ensures that it is orthogonal to I_2 and I_4 [51], so the key asymptotic behavior lies along I_1 and I_3 . As r_h approaches r_m and ∞ , the direction of ϕ shifts leftward, with an inclination that depends on the value of ϕ^Θ . In Table I, the direction pairs on the segments I_1 and I_3 , along with the topological number W , are listed for the four-dimensional Kerr black hole.

For the four-dimensional Kerr black hole, the topological number is $W = 0$. A generate point is found at $\beta_c/r_0 = 6\sqrt{3}\pi a$ [52], where r_0 is an arbitrary length scale determined by the size of a surrounding cavity. Below this point, no black hole states are present, indicating a trivial topology. At larger values of β , two black hole states—small and large—appear, with the former being thermodynamically stable and the latter unstable. The topological number always equals 0, regardless of the values of τ and the rotation parameter a .

Consider the variations in the components $(\phi^{r_h}, \phi^\Theta)$ of the vector ϕ for the four-dimensional Kerr black hole case along each contour depicted in Fig. 1, as illustrated in Fig. 2. The zero points of ϕ are located at the origin, and tracking the changes of ϕ along each C_i generates a closed loop Φ_i in the corresponding vector space. In Fig. 2, the direction of each contour reflects the rotation of ϕ as the associated contour in Fig. 1 is traversed counterclockwise. Contours with

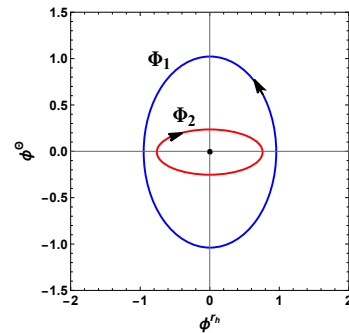


FIG. 2. Contours ϕ_i that represent changes in the components of the vector ϕ for the four-dimensional Kerr black hole are illustrated as C_i ($i = 1, 2$) in Fig. 1. The origin denotes the zero points of ϕ . The black arrows indicate the direction of rotation of the vector ϕ as it traverses each contour in Fig. 1. Along contour C_1 , the modifications in the components of ϕ cause the closed loop Φ_1 to follow a counterclockwise direction, resulting in a winding number of $+1$. Conversely, for contour C_2 , the behavior is reversed, yielding a winding number of -1 .

positive winding numbers in Fig. 1 are mapped to counterclockwise loops in Fig. 2, while those with negative winding numbers are mapped to clockwise loops. In the case of the four-dimensional Kerr black hole, the winding numbers of the first and second zero points are $+1$ and -1 , respectively.

Then, we analyze the systematic ordering for the four-dimensional Kerr black hole. There is at least one black hole state with positive heat capacity and a winding number of $+1$, and one black hole state with negative heat capacity and a winding number of -1 . If additional black hole states are present, they must emerge in pairs. As the signs of the heat capacities alternate with increasing r_h , the smallest state corresponds to a thermodynamically stable black hole, while the largest state corresponds to a thermodynamically unstable one. The winding numbers associated with the zero points follow the sequence $[+, (-, +), \dots, -]$, where the ellipsis represents pairs of $(+, -)$ winding numbers. For simplicity, the four-dimensional Kerr black hole case can be labeled as $[+, -]$ based on the signs of the innermost and outermost winding numbers.

In the following, we turn to discuss the universal thermodynamic behavior of the four-dimensional Kerr black hole. In the low-temperature limit, $\beta \rightarrow \infty$, the system features an unstable large black hole and a stable small black hole. At the high-temperature limit, $\beta \rightarrow 0$, no black hole state is present.

To summarize, based on the thermodynamic topological classification approach proposed in Ref. [96], the four-dimensional Kerr black hole falls under the class W^{0+} .

III. SINGLY ROTATING KERR BLACK HOLES IN ARBITRARY DIMENSIONS

In this section, we will extend the above discussion to rotating black holes in higher dimensions, specifically considering singly rotating Kerr black holes in d dimensions. The metric

for these black holes in arbitrary dimensions is expressed as [106, 107]

$$ds^2 = -\frac{\Delta_r}{\Sigma} \left(dt - a \sin^2 \theta d\phi \right)^2 + \frac{\Sigma}{\Delta_r} dr^2 + \Sigma d\theta^2 + \frac{\sin^2 \theta}{\Sigma} \left[a dt - (r^2 + a^2) d\phi \right]^2 + r^2 \cos^2 \theta d\Omega_{d-4}^2, \quad (11)$$

where $d\Omega_d$ represents the line element of a d -dimensional unit sphere, and

$$\Delta_r = r^2 + a^2 - 2mr^{5-d}, \quad \Sigma = r^2 + a^2 \cos^2 \theta.$$

The thermodynamic quantities are [107]

$$\begin{aligned} M &= \frac{d-2}{8\pi} \omega_{d-2} m, & J &= \frac{\omega_{d-2}}{4\pi} ma, \\ \Omega &= \frac{a}{r_h^2 + a^2}, & S &= \frac{\omega_{d-2}}{4} (r_h^2 + a^2) r_h^{d-4}, \\ T &= \frac{r_h}{2\pi} \left(\frac{1}{r_h^2 + a^2} + \frac{d-3}{2r_h^2} \right) - \frac{1}{2\pi r_h}, \end{aligned} \quad (12)$$

where $\omega_{d-2} = 2\pi^{(d-1)/2} / \Gamma[(d-1)/2]$, and the event horizon radius r_h of the black hole is determined by the largest root of the equation: $\Delta_{r_h} = 0$.

Next, we analyze the asymptotic behavior of the inverse temperature $\beta(r_h)$ for singly rotating Kerr black holes in different dimensions. For the case of the five-dimensional singly rotating Kerr black hole, its Hawking temperature approaches zero in two situations: one in the limit $r \rightarrow \infty$, and the other in the extremal case $r \rightarrow r_m = \sqrt{2m - a^2}$. However, for the cases of $d \geq 6$ singly rotating Kerr black holes, the Hawking temperature approaches zero in the limit $r \rightarrow \infty$, but it diverges as $r \rightarrow 0$. Thus, it yields two possibilities:

$$d = 5 \text{ case: } \beta(r_m) = \infty, \quad \beta(\infty) = \infty, \quad (13)$$

$$d \geq 6 \text{ cases: } \beta(r_m) = 0, \quad \beta(\infty) = \infty \quad (14)$$

for the asymptotic behaviour of the inverse temperature $\beta(r_h)$.

From Eq. (12), one can calculate the generalized free energy as

$$\begin{aligned} \mathcal{F} &= M - \frac{S}{\tau} \\ &= \frac{\omega_{d-2}(d-2)(r_h^2 + a^2)}{16\pi r_h^{5-d}} - \frac{\omega_{d-2}(r_h^2 + a^2)r_h^{d-4}}{4\tau}. \end{aligned} \quad (15)$$

Therefore the components of the vector ϕ can be computed as

$$\begin{aligned} \phi^{r_h} &= \frac{\omega_{d-2} r_h^{d-6}}{16\pi\tau} \left\{ (d-2) [(d-3)\tau - 4\pi r_h] r_h^2 \right. \\ &\quad \left. + a^2 [\tau(d-2)(d-5) - 4(d-4)\pi r_h] \right\}, \end{aligned} \quad (16)$$

$$\phi^\Theta = -\cot \Theta \csc \Theta. \quad (17)$$

We now analyze the asymptotic behavior of the vector ϕ at the boundary corresponding to Eqs. (13) and (14), which is also described by the contour $C = I_1 \cup I_2 \cup I_3 \cup I_4$ that covers

TABLE II. The direction indicated by the arrows of ϕ^{r_h} and the corresponding topological number for the $d \geq 5$ singly rotating Kerr black holes.

Black hole solutions	I_1	I_2	I_3	I_4	W
$d = 5$ singly rotating Kerr black hole	\leftarrow	\uparrow	\leftarrow	\downarrow	0
$d \geq 6$ singly rotating Kerr black hole	\leftarrow	\uparrow	\rightarrow	\downarrow	-1

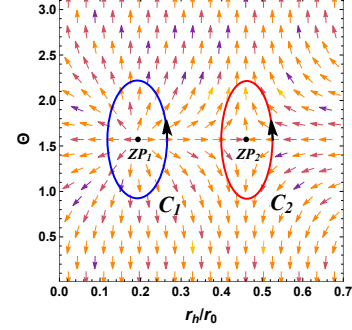


FIG. 3. The arrows represent the unit vector field on a portion of the $r_h - \Theta$ plane for the five-dimensional singly rotating Kerr black hole with $\beta/r_0 = 4$ and $a/r_0 = 0.5$. The zero points (ZPs) marked with black dots are at $(r_h/r_0, \Theta) = (0.19, \pi/2)$, and $(0.45, \pi/2)$, for ZP_1 , and ZP_2 , respectively. The blue contours C_i are closed loops surrounding the zero points.

all relevant parameter regions. In Table II, the direction pairs on segments I_1 and I_3 , as well as the topological number W , are provided for the $d \geq 5$ singly rotating Kerr black holes.

Based on the conclusions in our previous work [52], the topological numbers of the five-dimensional singly rotating Kerr black holes differ from those of the $d \geq 6$ singly rotating Kerr black holes. Therefore, we will next discuss the universal thermodynamic topological classification and related properties of the five-dimensional singly rotating Kerr black holes and the $d \geq 6$ singly rotating Kerr black holes separately.

A. $d = 5$ case

In this subsection, we focus on the case of the five-dimensional singly rotating Kerr black hole. For the $d = 5$ singly rotating Kerr black hole, the topological number is $W = 0$. A critical generation point occurs at $\beta_c/r_0 = 4\sqrt{3}\pi a/3$ [52], below which no black hole states exist, indicating trivial topology. At higher values of β , two black hole states, small and large, appear. The small black hole is thermodynamically stable, while the large one is unstable.

Examine the behavior of the components $(\phi^{r_h}, \phi^\Theta)$ of the vector ϕ for the five-dimensional singly rotating Kerr black hole along each contour shown in Fig. 3. This behavior is depicted in Fig. 4. For this five-dimensional case, the winding numbers of the first and second zero points are $+1$ and -1 , respectively, which are the same as the winding numbers for the four-dimensional Kerr black hole in the previous section.

We now examine the systematic ordering for the five-dimensional singly rotating Kerr black hole. It is observed that

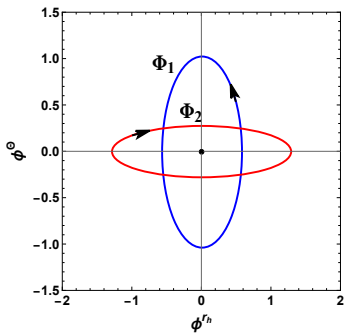


FIG. 4. Contours ϕ_i , representing changes in the components of the vector ϕ for the five-dimensional singly rotating Kerr black hole, are shown as C_i ($i = 1, 2$) in Fig. 3. The origin denotes the zero points of ϕ . Black arrows indicate the direction of rotation of the vector ϕ around each contour in Fig. 3. For contour C_1 , the changes in the components of ϕ cause the closed loop Φ_1 to move counterclockwise, resulting in a winding number of $+1$. In contrast, for contour C_2 , the movement is clockwise, giving a winding number of -1 .

there exists at least one black hole state with positive heat capacity and a winding number of $+1$, and one black hole state with negative heat capacity and a winding number of -1 . For clarity, the five-dimensional singly rotating Kerr black hole can be classified as $[+, -]$ according to the signs of the innermost and outermost winding numbers.

We next address the universal thermodynamic behavior of the five-dimensional singly rotating Kerr black hole. In the low temperature limit, $\beta \rightarrow \infty$, the configuration features an unstable large black hole and a stable small black hole. In contrast, at high temperatures ($\beta \rightarrow 0$), no black hole states are observed.

In summary, according to the thermodynamic topological classification method outlined in Ref. [96], the five-dimensional singly rotating Kerr black hole is categorized as W^{0+} .

B. $d \geq 6$ cases

In this subsection, we turn to focus on the cases of the $d \geq 6$ singly rotating Kerr black hole. For these black holes, given a τ , there exists only one black hole state characterized by a negative heat capacity. This state has a local winding number of -1 , which is consistent with its global topological number of -1 .

As a specific example, we explore the behavior of the components $(\phi^{r_h}, \phi^\Theta)$ of the vector ϕ for the six-dimensional singly rotating Kerr black hole, analyzing each contour shown in Fig. 5 and illustrated in Fig. 6. It is worth noting that the behavior of the components $(\phi^{r_h}, \phi^\Theta)$ of the vector ϕ for the seven-, eight-, and nine-dimensional singly rotating Kerr black holes is similar to that of the six-dimensional singly rotating Kerr black hole. Thus, we will not plot them again here. Therefore, we can conclude that for the $d \geq 6$ singly rotating Kerr black hole, the winding number of the zero point is always -1 .

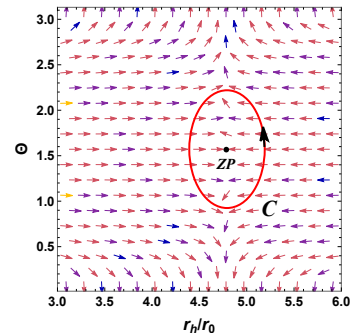


FIG. 5. The arrows represent the unit vector field on a portion of the $r_h - \Theta$ plane for the six-dimensional singly rotating Kerr black hole with $\beta/r_0 = 20$ and $a/r_0 = 0.5$. The zero point (ZP) marked with black dot is at $(r_h/r_0, \Theta) = (4.77, \pi/2)$. The blue contour C is closed loop surrounding the zero point.

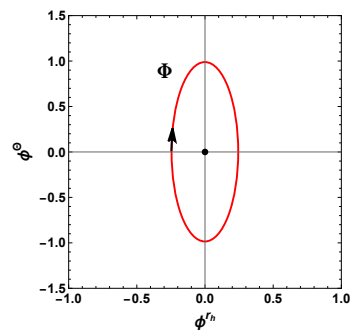


FIG. 6. Contours labeled ϕ_i , representing the variations in the components of the vector ϕ for the six-dimensional singly rotating Kerr black hole, are denoted as C in Fig. 5. The origin marks the zero point of ϕ . Black arrows illustrate the direction of the vector ϕ 's rotation around each contour in Fig. 5. For contour C , the changes in ϕ cause the closed loop Φ to trace a clockwise path, corresponding to a winding number of -1 .

Now, we analyze the systematic ordering for the $d \geq 6$ singly rotating Kerr black holes. It is easy to observe that there is at least one black hole state that possesses a negative heat capacity and a winding number of -1 . If additional black hole states exist, they must appear in pairs. The heat capacities alternate in sign with increasing r_h , with the smallest and largest states corresponding to thermodynamically unstable black holes. The winding numbers at the zero points follow the sequence $[-, (+, -), \dots, (+, -)]$. For simplicity, the singly rotating Kerr black hole in dimensions $d \geq 6$ can be characterized by $[-, -]$, indicating the signs of the innermost and outermost winding numbers.

Then, we investigate the universal thermodynamic behavior of the $d \geq 6$ singly rotating Kerr black holes. In the low-temperature limit, where $\beta \rightarrow \infty$, the system features a large black hole that is thermodynamically unstable. Conversely, in the high-temperature limit, where $\beta \rightarrow 0$, the system displays an unstable small black hole state.

To sum up, based on the thermodynamic topological classification approach detailed in Ref. [96], the singly rotating Kerr black hole in $d \geq 6$ dimensions is classified as W^{1-} .

IV. FOUR-DIMENSIONAL KERR-NEWMAN BLACK HOLE

Finally, in this section, we investigate the universal thermodynamic topological class of the four-dimensional Kerr-Newman black hole [108, 109]. Its metric and Abelian gauge potential are given by

$$ds^2 = -\frac{\Delta_r}{\Sigma} \left(dt - a \sin^2 \theta d\phi \right)^2 + \frac{\Sigma}{\Delta_r} dr^2 + \Sigma d\theta^2 + \frac{\sin^2 \theta}{\Sigma} [adt - (r^2 + a^2)d\phi]^2, \quad (18)$$

$$A = \frac{qr}{\Sigma} (dt - a \sin^2 \theta d\phi), \quad (19)$$

where

$$\Delta_r = r^2 + a^2 - 2mr + q^2, \quad \Sigma = r^2 + a^2 \cos^2 \theta.$$

Here, m is the mass parameter. The parameters a and q represent the rotation and electric charge, respectively.

The thermodynamic quantities are expressed as follows [104, 105]:

$$\begin{aligned} M &= m, & J &= ma, & \Omega &= \frac{a}{r_h^2 + a^2}, \\ Q &= q, & \Phi &= \frac{qr}{r_h^2 + a^2}, \\ S &= \pi(r_h^2 + a^2), & T &= \frac{r_h^2 - a^2 - q^2}{4\pi r_h(r_h^2 + a^2)}, \end{aligned} \quad (20)$$

where $r_h = m + \sqrt{m^2 - a^2 - q^2}$ is the location of the event horizon. The Hawking temperature of the four-dimensional Kerr-Newman black hole vanishes in both the limit $r \rightarrow \infty$ and the extremal horizon limit, where $r_m = m = \sqrt{a^2 + q^2}$.

As a result, the inverse temperature $\beta(r_h)$ reaches

$$\beta(r_m) = \infty, \quad \beta(\infty) = \infty \quad (21)$$

at these asymptotic boundaries.

Substituting $m = (r_h^2 + a^2 + q^2)/(2r_h)$ into the definition of the generalized Helmholtz free energy (1), one can arrive at

$$\mathcal{F} = \frac{r_h^2 + a^2 + q^2}{2r_h} - \frac{\pi(r_h^2 + a^2)}{\tau}, \quad (22)$$

and

$$\hat{\mathcal{F}} = \frac{r_h^2 + a^2 + q^2}{2r_h} - \frac{\pi(r_h^2 + a^2)}{\tau} + \frac{1}{\sin \Theta}. \quad (23)$$

Thus, the components of the vector ϕ are

$$\phi^{r_h} = 1 - \frac{r_h^2 + a^2 + q^2}{2r_h^2} - \frac{2\pi r_h}{\tau}, \quad (24)$$

$$\phi^\Theta = -\cot \Theta \csc \Theta. \quad (25)$$

The asymptotic behavior of the vector ϕ at the boundary associated with Eq. (21) is examined, with the contour $C =$

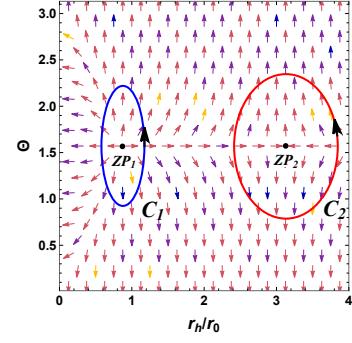


FIG. 7. The arrows represent the unit vector field on a portion of the $r_h - \Theta$ plane for the four-dimensional Kerr-Newman black hole with $\beta/r_0 = 40$, $a/r_0 = 0.5$ and $q/r_0 = 0.5$. The zero points (ZPs) marked with black dots are at $(r_h/r_0, \Theta) = (0.82, \pi/2)$, and $(3.01, \pi/2)$, for ZP_1 , and ZP_2 , respectively. The blue contours C_i are closed loops surrounding the zero points.

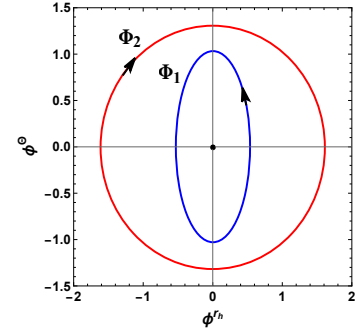


FIG. 8. Contours ϕ_i , representing changes in the vector components for the four-dimensional Kerr-Newman black hole, are illustrated in Fig. 7 as C_i ($i = 1, 2$). The origin marks the zero points of ϕ . Black arrows indicate the rotation of the vector ϕ along each contour. For C_1 , the changes in ϕ lead to a counterclockwise rotation of the closed loop Φ_1 , producing a winding number of $+1$. In contrast, for C_2 , the loop rotates clockwise, giving a winding number of -1 .

$I_1 \cup I_2 \cup I_3 \cup I_4$ describing this behavior and encompassing all relevant parameter regions. Table III presents the direction pairs for segments I_1 and I_3 , as well as the topological number W for the four-dimensional Kerr-Newman black hole.

For the four-dimensional Kerr-Newman black hole, the topological number is $W = 0$. A generation point is found at $\beta_c/r_0 = 6\pi\sqrt{3}(a^2 + q^2)$ [52]. Below this point, no black hole states exist, reflecting a trivial topology. At higher values of β , two black hole states emerge: a small, thermodynamically stable state and a large, unstable one. The topological number remains zero regardless of the values of τ , the rotation parameter a , or the electric charge parameter q .

TABLE III. The direction indicated by the arrows of ϕ^{r_h} and the corresponding topological number for the four-dimensional Kerr-Newman black hole.

Black hole solutions	I_1	I_2	I_3	I_4	W
$d = 4$ Kerr-Newman black hole	\leftarrow	\uparrow	\leftarrow	\downarrow	0

The behavior of the vector components $(\phi^{r_h}, \phi^\Theta)$ for the four-dimensional Kerr-Newman black hole is examined along each contour in Fig. 7. This behavior is illustrated in Fig. 8. In this case, the winding numbers at the first and second zero points are $+1$ and -1 , respectively, which match those found for the four-dimensional Kerr black hole in Sec. II.

We now investigate the systematic ordering for the four-dimensional Kerr-Newman black hole. It is demonstrated that there is always at least one black hole state with a positive heat capacity and a winding number of $+1$. Additionally, there is at least one state with a negative heat capacity and a winding number of -1 . Therefore, the four-dimensional black hole is classified as $[+, -]$ based on the signs of its innermost and outermost winding numbers.

Next, we consider the universal thermodynamic behavior of the four-dimensional Kerr-Newman black hole. In the low-temperature limit, $\beta \rightarrow \infty$, the configuration consists of a stable small black hole and an unstable large black hole, respectively. At high temperatures ($\beta \rightarrow 0$), the black hole states disappear entirely.

In conclusion, following the thermodynamic topological classification method described in Ref. [96], the four-dimensional Kerr-Newman black hole is classified as W^{0+} .

V. CONCLUSIONS AND OUTLOOKS

Our results found in the present paper are now summarized in the following Table IV.

In this paper, we explore the universal thermodynamic topological classification of singly rotating Kerr black holes in arbitrary dimensions, as well as the four-dimensional Kerr-Newman black hole. We find that the innermost small black hole states of the singly rotating Kerr black holes with $d \geq 6$ are thermodynamically unstable. In contrast, the corresponding states of the four-dimensional Kerr-Newman black hole and the $d = 4, 5$ singly rotating Kerr black holes are thermodynamically stable. Additionally, the outermost large black holes are unstable in all cases.

At low temperatures, the $d \geq 6$ singly rotating Kerr black holes feature a single large, thermodynamically unstable black hole. In contrast, the four-dimensional Kerr-Newman black hole and the $d = 4, 5$ singly rotating Kerr black holes exhibit one large unstable branch and one small stable branch. At high temperatures, the $d \geq 6$ singly rotating Kerr black holes show a small, unstable black hole state, while the four-dimensional Kerr-Newman black hole and the $d = 4, 5$ singly rotating Kerr black holes have no black hole states.

As a result, we conclude that the singly rotating Kerr black holes with $d \geq 6$ are classified as W^{1-} , while the four-dimensional Kerr-Newman black hole and the $d = 4, 5$ singly rotating Kerr black holes with are classified as W^{0+} . This find-

ing also supports the conjecture proposed in Ref. [96], which suggests that black hole solutions should be categorized into four distinct classes based on their universal thermodynamic topological properties.

A particularly intriguing issue is to delve deeper into the universal thermodynamic topological properties of black holes with unusual horizon topologies. These include planar [110], toroidal [111], hyperbolic [112], and ultraspinning black holes [113–122], as well as NUT-charged spacetimes [123–127] and type-D NUT C-metric black holes [128], etc. We believe that this could help elucidate the connections between horizon topology and thermodynamic topology.

ACKNOWLEDGMENTS

We are greatly indebted to the anonymous referee for the constructive comments to improve the presentation of this work. This work is supported by the National Natural Science Foundation of China (NSFC) under Grants No. 12205243, No. 12375053, by the Sichuan Science and Technology Program under Grant No. 2023NSFSC1347, by the Doctoral Research Initiation Project of China West Normal University under Grant No. 21E028, and by the Postgraduate Scientific Research Innovation Project of Hunan Province under Grant No. CX20240531.

Appendix A: Four thermodynamic topological classes

According to Ref. [96], the four topological classes of black hole thermodynamics are:

$$W^{1-}, W^{0+}, W^{0-}, W^{1+}, \quad (\text{A1})$$

These classes correspond to distinct asymptotic behaviors of the inverse temperature $\beta(r_h)$:

$$W^{1-} : \beta(r_m) = 0, \quad \beta(\infty) = \infty, \quad (\text{A2})$$

$$W^{0+} : \beta(r_m) = \infty, \quad \beta(\infty) = \infty, \quad (\text{A3})$$

$$W^{0-} : \beta(r_m) = 0, \quad \beta(\infty) = 0, \quad (\text{A4})$$

$$W^{1+} : \beta(r_m) = \infty, \quad \beta(\infty) = 0, \quad (\text{A5})$$

where r_m represents the minimal radius of the black hole event horizon, which may or may not be zero. For instance, in the extremal case of a Reissner-Nordström (RN) black hole with a fixed charge Q , we have $r_m = M = Q = r_e$. In contrast, a Schwarzschild black hole has r_m equal to zero. Table V summarizes the properties of these four topological classes, thereby enhancing our understanding of their distinct characteristics.

[1] P.V.P. Cunha, C.A.R. Herdeiro, E. Radu, and H.F. Runarsson, Shadows of Kerr black holes with scalar hair, *Phys. Rev.*

TABLE IV. The universal thermodynamic topological classifications of the rotating black holes and their thermodynamical properties. Here and hereafter, DP, AP, and GP represent the degenerate point, annihilation point, and generation point, respectively.

BH solutions	Innermost	Outermost	Low T	High T	DP	W	Classes
$d = 4$ Kerr BH	stable	unstable	unstable large + stable small	no	one more GP	0	W^{0+}
$d = 4$ Kerr-Newman BH	stable	unstable	unstable large + stable small	no	one more GP	0	W^{0+}
$d = 5$ singly rotating Kerr BH	stable	unstable	unstable large + stable small	no	one more GP	0	W^{0+}
$d \geq 6$ singly rotating Kerr BH	unstable	unstable	unstable large	unstable small	in pairs	-1	W^{1-}

TABLE V. Thermodynamical properties of the black hole states for the four topological classes of W^{1-} , W^{0+} , W^{0-} , and W^{1+} , respectively.

Classes	Innermost	Outermost	Low T	High T	DP	W	Typical cases
W^{1-}	unstable	unstable	unstable large	unstable small	in pairs	-1	Schwarzschild BH
W^{0+}	stable	unstable	unstable large+stable small	no	one more GP	0	RN BH
W^{0-}	unstable	stable	no	unstable small+stable large	one more AP	0	Schwarzschild-AdS BH
W^{1+}	stable	stable	stable small	stable large	in pairs	+1	RN-AdS BH

- [2] A. Grenzebach, V. Perlick, and C. Lämmerzahl, Photon regions and shadows of Kerr-Newman-NUT black holes with a cosmological constant, *Phys. Rev. D* **89**, 124004 (2014).
- [3] S. Vagnozzi *et al.*, Horizon-scale tests of gravity theories and fundamental physics from the Event Horizon Telescope image of Sagittarius A*, *Classical Quantum Gravity* **40**, 165007 (2023).
- [4] W. Liu, D. Wu, X. Fang, J. Jing, and J. Wang, Kerr-MOG-(A)dS black hole and its shadow in scalar-tensor-vector gravity theory, *J. Cosmol. Astropart. Phys.* **08** (2024) 035.
- [5] W. Liu, D. Wu, and J. Wang, Shadow of slowly rotating Kalb-Ramond black holes, [arXiv:2407.07416](https://arxiv.org/abs/2407.07416).
- [6] The Event Horizon Telescope Collaboration, First M87 Event Horizon Telescope Results. I. The Shadow of the Supermassive Black Hole, *Astrophys. J. Lett.* **875**, L1 (2019).
- [7] The Event Horizon Telescope Collaboration, First Sagittarius A* Event Horizon Telescope Results. I. The Shadow of the Supermassive Black Hole in the Center of the Milky Way, *Astrophys. J. Lett.* **930**, L12 (2022).
- [8] B.P. Abbott *et al.* (LIGO Scientific and Virgo Collaborations), Observation of Gravitational Waves from a Binary Black Hole Merger, *Phys. Rev. Lett.* **116**, 061102 (2016).
- [9] B.P. Abbott *et al.* (LIGO Scientific and Virgo Collaborations), GW151226: Observation of Gravitational Waves from a 22-Solar-Mass Binary Black Hole Coalescence, *Phys. Rev. Lett.* **116**, 241103 (2016).
- [10] P.V.P. Cunha, E. Berti, and C.A.R. Herdeiro, Light Ring Stability in Ultra-Compact Objects, *Phys. Rev. Lett.* **119**, 251102 (2017).
- [11] P.V.P. Cunha, and C.A.R. Herdeiro, Stationary Black Holes and Light Rings, *Phys. Rev. Lett.* **124**, 181101 (2020).
- [12] S.-W. Wei, Topological charge and black hole photon spheres, *Phys. Rev. D* **102**, 0604039 (2020).
- [13] M. Guo and S. Gao, Universal properties of light rings for stationary axisymmetric spacetimes, *Phys. Rev. D* **103**, 104031 (2021).
- [14] R. Ghosh and S. Sarkar, Light rings of stationary spacetimes, *Phys. Rev. D* **104**, 044019 (2021).
- [15] M. Guo, Z. Zhong, J. Wang, and S. Gao, Light rings and long-lived modes in quasiblack hole spacetimes, *Phys. Rev. D* **105**, 024049 (2022).
- [16] H.C.D.L. Junior, J.-Z. Yang, L.C.B. Crispino, P.V.P. Cunha, and C.A.R. Herdeiro, Einstein-Maxwell-dilaton neutral black holes in strong magnetic fields: Topological charge, shadows, and lensing, *Phys. Rev. D* **105**, 064070 (2022).
- [17] S.-P. Wu and S.-W. Wei, Topology of light rings for extremal and nonextremal Kerr-Newman-Taub-NUT black holes without Z_2 symmetry, *Phys. Rev. D* **108**, 104041 (2023).
- [18] P.V.P. Cunha, C.A.R. Herdeiro, and J.P.A. Novo, Light rings on stationary axisymmetric spacetimes: blind to the topology and able to coexist, *Phys. Rev. D* **109**, 064050 (2024).
- [19] W. Liu, D. Wu, and J. Wang, Light rings and shadows of static black holes in effective quantum gravity, *Phys. Lett. B* **858**, 139052 (2024).
- [20] S.-W. Wei and Y.-X. Liu, Topology of equatorial timelike circular orbits around stationary black holes, *Phys. Rev. D* **107**, 064006 (2023).
- [21] X. Ye and S.-W. Wei, Topological study of equatorial timelike circular orbit for spherically symmetric (hairy) black holes, *J. Cosmol. Astropart. Phys.* **07** (2023) 049.
- [22] X. Ye and S.-W. Wei, Novel topological phenomena of timelike circular orbits for charged test particles, [arXiv:2406.13270](https://arxiv.org/abs/2406.13270).
- [23] S.-W. Wei and Y.-X. Liu, Topology of black hole thermodynamics, *Phys. Rev. D* **105**, 104003 (2022).
- [24] P.K. Yerra and C. Bhamidipati, Topology of black hole thermodynamics in Gauss-Bonnet gravity, *Phys. Rev. D* **105**, 104053 (2022).
- [25] P.K. Yerra and C. Bhamidipati, Topology of Born-Infeld AdS black holes in 4D novel Einstein-Gauss-Bonnet gravity. *Phys. Lett. B* **835**, 137591 (2022).
- [26] M.B. Ahmed, D. Kubiznak, and R.B. Mann, Vortex/anti-vortex pair creation in black hole thermodynamics, *Phys. Rev. D* **107**, 046013 (2023).
- [27] N.J. Gogoi and P. Phukon, Topology of thermodynamics in R -charged black holes, *Phys. Rev. D* **107**, 106009 (2023).
- [28] M. Zhang and J. Jiang, Bulk-boundary thermodynamic equivalence: a topology viewpoint, *J. High Energy Phys.* **06** (2023) 115.
- [29] M.R. Alipour, M.A.S. Afshar, S.N. Gashti, and J. Sadeghi, Topological classification and black hole thermodynamics, *Phys. Dark Univ.* **42**, 101361 (2023).
- [30] Z.-M. Xu, Y.-S. Wang, B. Wu, and W.-L. Yang, Riemann surface, winding number and black hole thermodynamics, *Phys. Lett. B* **850**, 138528 (2024).

- [31] M.-Y. Zhang, H. Chen, H. Hassanabadi, Z.-W. Long, and H. Yang, Topology of nonlinearly charged black hole chemistry via massive gravity, *Eur. Phys. J. C* **83**, 773 (2023).
- [32] T.N. Hung and C.H. Nam, Topology in thermodynamics of regular black strings with Kaluza-Klein reduction, *Eur. Phys. J. C* **83**, 582 (2023).
- [33] J. Sadeghi, M.R. Alipour, S.N. Gashti, and M.A.S. Afshar, Bulk-boundary and RPS thermodynamics from topology perspective, *Chin. Phys. C* **48**, 095106 (2024).
- [34] P.K. Yerra, C. Bhamidipati and S. Mukherji, Topology of critical points and Hawking-Page transition, *Phys. Rev. D* **106**, 064059 (2022).
- [35] Z.-Y. Fan, Topological interpretation for phase transitions of black holes, *Phys. Rev. D* **107**, 044026 (2023).
- [36] N.-C. Bai, L. Li and J. Tao, Topology of black hole thermodynamics in Lovelock gravity, *Phys. Rev. D* **107**, 064015 (2023).
- [37] N.-C. Bai, L. Song, and J. Tao, Reentrant phase transition in holographic thermodynamics of Born-Infeld AdS black hole, *Eur. Phys. J. C* **84**, 43 (2024).
- [38] R. Li, C.H. Liu, K. Zhang, and J. Wang, Topology of the landscape and dominant kinetic path for the thermodynamic phase transition of the charged Gauss-Bonnet AdS black holes, *Phys. Rev. D* **108**, 044003 (2023).
- [39] P.K. Yerra, C. Bhamidipati, and S. Mukherji, Topology of critical points in boundary matrix duals, *J. High Energy Phys.* **03** (2024) 138.
- [40] Y.-Z. Du, H.-F. Li, Y.-B. Ma, and Q. Gu, Topology and phase transition for EPYM AdS black hole in thermal potential, *Nucl. Phys. B* **1006**, 116641 (2024).
- [41] P.K. Yerra, C. Bhamidipati, and S. Mukherji, Topology of Hawking-Page transition in Born-Infeld AdS black holes, *J. Phys. Conf. Ser.* **2667**, 012031 (2023).
- [42] K. Bhattacharya, K. Bamba, and D. Singleton, Topological interpretation of extremal and Davies-type phase transitions of black holes, *Phys. Lett. B* **854**, 138722 (2024).
- [43] H. Chen, M.-Y. Zhang, H. Hassanabadi, B.C. Lutfuoglu, and Z.-W. Long, Topology of dyonic AdS black holes with quasitopological electromagnetism in Einstein-Gauss-Bonnet gravity, [arXiv:2403.14730](https://arxiv.org/abs/2403.14730).
- [44] B. Hazarika, N.J. Gogoi, and P. Phukon, Revisiting thermodynamic topology of Hawking-Page and Davies type phase transitions, [arXiv:2404.02526](https://arxiv.org/abs/2404.02526).
- [45] T.N. Hung and C.H. Nam, Topological equivalence and phase transition rate in holographic thermodynamics of regularized Maxwell theory, *Eur. Phys. J. C* **84**, 870 (2024).
- [46] I. Jeon, B.-H. Lee, W. Lee, and M. Mishra, Stability and topological nature of charged Gauss-Bonnet AdS black holes in five dimensions, [arXiv:2407.20016](https://arxiv.org/abs/2407.20016).
- [47] H. Chen, M.Y. Zhang, A.A.A. Filho, F. Hosseinifar, and H. Hassanabadi, Thermal, topological, and scattering effects of an AdS charged black hole with an antisymmetric tensor background, [arXiv:2408.03090](https://arxiv.org/abs/2408.03090).
- [48] J. Sadeghi, M.R. Alipour, M.A.S. Afshar, and S.N. Gashti, Exploring the phase transition in charged Gauss-Bonnet black holes: a holographic thermodynamics perspectives, *Gen. Rel. Grav.* **56**, 93 (2024).
- [49] A. Mehmood, N. Alessa, M.U. Shahzad, and E.E. Zotos, Davies-type phase transitions in 4D Dyonic AdS black holes from topological perspective, *Nucl. Phys. B* **1006**, 116653 (2024).
- [50] F. Barzi, H.E. Mousni, and K. Masmar, Riemann surfaces and winding numbers of Renyi phase structure of charged-flat black holes, [arXiv:2408.05870](https://arxiv.org/abs/2408.05870).
- [51] S.-W. Wei, Y.-X. Liu, and R.B. Mann, Black Hole Solutions as Topological Thermodynamic Defects, *Phys. Rev. Lett.* **129**, 191101 (2022).
- [52] D. Wu, Topological classes of rotating black holes, *Phys. Rev. D* **107**, 024024 (2023).
- [53] D. Wu and S.-Q. Wu, Topological classes of thermodynamics of rotating AdS black holes, *Phys. Rev. D* **107**, 084002 (2023).
- [54] D. Wu, Classifying topology of consistent thermodynamics of the four-dimensional neutral Lorentzian NUT-charged spacetimes, *Eur. Phys. J. C* **83**, 365 (2023).
- [55] D. Wu, Consistent thermodynamics and topological classes for the four-dimensional Lorentzian charged Taub-NUT spacetimes, *Eur. Phys. J. C* **83**, 589 (2023).
- [56] D. Wu, Topological classes of thermodynamics of the four-dimensional static accelerating black holes, *Phys. Rev. D* **108**, 084041 (2023).
- [57] D. Wu, S.-Y. Gu, X.-D. Zhu, Q.-Q. Jiang, and S.-Z. Yang, Topological classes of the thermodynamics of the static multi-charge AdS black holes in gauged supergravities: novel temperature-dependent thermodynamic topological phase transition, *J. High Energy Phys.* **06** (2024) 213.
- [58] X.-D. Zhu, D. Wu, and D. Wen, Topological classes of thermodynamics of the rotating charged AdS black holes in gauged supergravities, *Phys. Lett. B* **856**, 138919 (2024).
- [59] H. Chen, D. Wu, M.-Y. Zhang, H. Hassanabadi, and Z.-W. Long, Thermodynamic topology of phantom AdS black holes in massive gravity, *Phys. Dark Univ.* **46**, 101617 (2024).
- [60] W. Liu, L. Zhang, D. Wu, and J. Wang, Thermodynamic topological classes of the rotating, accelerating black holes, [arXiv:2409.11666](https://arxiv.org/abs/2409.11666).
- [61] C.H. Liu and J. Wang, The topological natures of the Gauss-Bonnet black hole in AdS space, *Phys. Rev. D* **107**, 064023 (2023).
- [62] C.X. Fang, J. Jiang and M. Zhang, Revisiting thermodynamic topologies of black holes, *J. High Energy Phys.* **01** (2023) 102.
- [63] N. Chatzifotis, P. Dorlis, N.E. Mavromatos, and E. Papanonopoulos, Thermal stability of hairy black holes, *Phys. Rev. D* **107**, 084053 (2023).
- [64] S.-W. Wei, Y.-P. Zhang, Y.-X. Liu, and R.B. Mann, Implementing static Dyson-like spheres around spherically symmetric black hole, *Phys. Rev. Res.* **5**, 043050 (2023).
- [65] Y. Du and X. Zhang, Topological classes of black holes in de-Sitter spacetime, *Eur. Phys. J. C* **83**, 927 (2023).
- [66] C. Fairros and T. Sharqui, *Int. J. Mod. Phys. A* **38**, 2350133 (2023).
- [67] D. Chen, Y. He, and J. Tao, Thermodynamic topology of higher-dimensional black holes in massive gravity, *Eur. Phys. J. C* **83**, 872 (2023).
- [68] N.J. Gogoi and P. Phukon, Thermodynamic topology of 4d dyonic AdS black holes in different ensembles, *Phys. Rev. D* **108**, 066016 (2023).
- [69] J. Sadeghi, S.N. Gashti, M.R. Alipour, and M.A.S. Afshar, Bardeen black hole thermodynamics from topological perspective, *Ann. Phys. (Amsterdam)* **455**, 169391 (2023).
- [70] M.S. Ali, H.E. Mousni, J. Khalloufi, and K. Masmar, Topology of Born-Infeld-AdS black hole phase transition, *Ann. Phys. (Amsterdam)* **465**, 169679 (2024).
- [71] J. Sadeghi, M.A.S. Afshar, S.N. Gashti, and M.R. Alipour, Thermodynamic topology and photon spheres in the hyper-scaling violating black holes, *Astropart. Phys.* **156**, 102920 (2024).
- [72] F. Barzi, H.E. Mousni, and K. Masmar, Rényi topology of charged-flat black hole: Hawking-Page and Van-der-Waals phase transitions, *JHEAp* **42**, 63 (2024).

- [73] M.U. Shahzad, A. Mehmood, S. Sharif, and A. Övgün, Criticality and topological classes of neutral Gauss-Bonnet AdS black holes in 5D, *Ann. Phys. (Amsterdam)* **458**, 169486 (2023).
- [74] C.-W. Tong, B.-H. Wang, and J.-R. Sun, Topology of black hole thermodynamics via Rényi statistics, *Eur. Phys. J. C* **84**, 826 (2024).
- [75] M. Rizwan and K. Jusufi, Topological classes of thermodynamics of black holes in perfect fluid dark matter background, *Eur. Phys. J. C* **83**, 944 (2023).
- [76] C. Fairros, Topological interpretation of black hole phase transition in Gauss-Bonnet gravity, *Int. J. Mod. Phys. A* **39**, 2450030 (2024).
- [77] D. Chen, Y. He, J. Tao, and W. Yang, Topology of Hořava-Lifshitz black holes in different ensembles, *Eur. Phys. J. C* **84**, 96 (2024).
- [78] J. Sadeghi, M.A.S. Afshar, S.N. Gashti, and M.R. Alipour, Thermodynamic topology of black holes from bulk-boundary, extended, and restricted phase space perspectives, *Ann. Phys. (Amsterdam)* **460**, 169569 (2023).
- [79] B. Hazarika and P. Phukon, Thermodynamic topology of $D = 4, 5$ Horava Lifshitz black hole in two ensembles, *Nucl. Phys. B* **1006**, 116649 (2024).
- [80] N.J. Gogoi and P. Phukon, Thermodynamic topology of 4D Euler-Heisenberg-AdS black hole in different ensembles, *Phys. Dark Univ.* **44**, 101456 (2024).
- [81] M.-Y. Zhang, H. Chen, H. Hassanabadi, Z.-W. Long, and H. Yang, Thermodynamic topology of Kerr-Sen black holes via Rényi statistics, *Phys. Lett. B* **856**, 138885 (2024).
- [82] J. Sadeghi, M.A.S. Afshar, S.N. Gashti, and M.R. Alipour, Topology of Hayward-AdS black hole thermodynamics, *Phys. Scripta* **99**, 025003 (2024).
- [83] B. Hazarika and P. Phukon, Thermodynamic topology of black holes in $f(R)$ gravity, *PETP* **2024**, 043E01 (2024).
- [84] A. Malik, A. Mehmood, and M.U. Shahzad, Thermodynamic topological classification of higher dimensional and massive gravity black holes, *Ann. Phys. (Amsterdam)* **463**, 169617 (2024).
- [85] M.U. Shahzad, A. Mehmood, A. Malik, and A. Övgün, Topological behavior of 3D regular black hole with zero point length, *Phys. Dark Univ.* **44**, 101437 (2024).
- [86] S.-P. Wu and S.-W. Wei, Thermodynamical topology of quantum BTZ black hole, *Phys. Rev. D* **110**, 024054 (2024).
- [87] B. Hazarika and P. Phukon, Topology of restricted phase space thermodynamics in Kerr-Sen-AdS black holes, [arXiv:2405.02328](https://arxiv.org/abs/2405.02328).
- [88] Z.-Q. Chen and S.-W. Wei, Thermodynamical topology with multiple defect curves for dyonic AdS black holes, [arXiv:2405.07525](https://arxiv.org/abs/2405.07525).
- [89] B.E. Panah, B. Hazarika, and P. Phukon, Thermodynamic topology of topological black hole in $F(R)$ -ModMax gravity's rainbow, *PETP* **2024**, 083E02 (2024).
- [90] H. Wang and Y.-Z. Du, Topology of the charged AdS black hole in restricted phase space, *Chin. Phys. C* **48**, 095109 (2024).
- [91] A.S. Mohamed and E.E. Zotos, Motion of test particles and topological interpretation of generic rotating regular black holes coupled to non-linear electrodynamics, *Astron. Comput.* **48**, 100853 (2024).
- [92] B. Hazarika, B.E. Panah, and P. Phukon, Thermodynamic topology of topological charged dilatonic black holes, [arXiv:2407.05325](https://arxiv.org/abs/2407.05325).
- [93] Bi. Hazarika, A. Bhattacharjee, and P. Phukon, Thermodynamics of rotating AdS black holes in Kaniadakis statistics, [arXiv:2408.08325](https://arxiv.org/abs/2408.08325).
- [94] Y. Sekhmani, S.N. Gashti, M.A.S. Afshar, M.R. Alipour, J. Sadeghi, and J. Rayimbaev, Thermodynamic topology of Black Holes in $F(R)$ -Euler-Heisenberg gravity's Rainbow, [arXiv:2409.04997](https://arxiv.org/abs/2409.04997).
- [95] M.U. Shahzad, A. Mehmood, and Ali Övgün, Thermodynamic topological classification of D-dimensional dyonic AdS black holes with quasitopological electromagnetism in Einstein-Gauss-Bonnet gravity, *Eur. Phys. J. Plus* **139**, 806 (2024).
- [96] S.-W. Wei, Y.-X. Liu, and R.B. Mann, Universal topological classifications of black hole thermodynamics, *Phys. Rev. D* **110**, L081501 (2024).
- [97] R. Li and J. Wang, Generalized free energy landscape of a black hole phase transition, *Phys. Rev. D* **106**, 106015 (2022).
- [98] G.W. Gibbons and S.W. Hawking, Action integrals and partition functions in quantum gravity, *Phys. Rev. D* **15**, 2752 (1977).
- [99] J.W. York, Black-hole thermodynamics and the Euclidean Einstein action, *Phys. Rev. D* **33**, 2092 (1986).
- [100] Y.-S. Duan and M.-L. Ge, $SU(2)$ gauge theory and electrodynamics of N moving magnetic monopoles, *Sci. Sin.* **9**, 1072 (1979).
- [101] Y.-S. Duan, S. Li, and G.-H. Yang, The bifurcation theory of the Gauss-Bonnet-Chern topological current and Morse function, *Nucl. Phys. B* **514**, 705 (1998).
- [102] L.-B. Fu, Y.-S. Duan, and H. Zhang, Evolution of the Chern-Simons vortices, *Phys. Rev. D* **61**, 045004 (2000).
- [103] B. Carter, Hamilton-Jacobi and Schrodinger separable solutions of Einstein's equations, *Commun. Math. Phys.* **10**, 280 (1968).
- [104] J.M. Bardeen, B. Carter, and S.W. Hawking, The four laws of black hole mechanics, *Commun. Math. Phys.* **31**, 161 (1973).
- [105] L. Smarr, Mass formula for Kerr black holes, *Phys. Rev. Lett.* **30**, 71 (1973); Erratum, **30**, 521 (1973).
- [106] R.C. Myers and M.J. Perry, Black holes in higher dimensional space-times, *Ann. Phys. (N.Y.)* **172**, 304 (1986).
- [107] S.-W. Wei, P. Cheng, and Y.-X. Liu, Analytical and exact critical phenomena of d -dimensional singly spinning Kerr-AdS black holes, *Phys. Rev. D* **93**, 084015 (2016).
- [108] E.T. Newman and A.I. Janis, Note on the Kerr spinning particle metric, *J. Math. Phys. (N.Y.)* **6**, 915 (1965).
- [109] E.T. Newman, E. Couch, K. Chinnapared, A. Exton, A. Prakash, and R. Torrence, Metric of a rotating, charged mass, *J. Math. Phys. (N.Y.)* **6**, 918 (1965).
- [110] R.G. Cai and Y.Z. Zhang, Black plane solutions in four-dimensional space-times, *Phys. Rev. D* **54**, 4891 (1996).
- [111] D.R. Brill and J. Louko, Thermodynamics of $(3+1)$ -dimensional black holes with toroidal or higher genus horizons, *Phys. Rev. D* **56**, 3600 (1997).
- [112] Y. Chen, Y.K. Lim, and E. Teo, Deformed hyperbolic black holes, *Phys. Rev. D* **92**, 044058 (2015).
- [113] D. Klemm, Four-dimensional black holes with unusual horizons, *Phys. Rev. D* **89**, 084007 (2014).
- [114] R.A. Hennigar, R.B. Mann, and D. Kubiznak, Entropy Inequality Violations from Ultraspinning Black Holes, *Phys. Rev. Lett.* **115**, 031101 (2015).
- [115] A. Gneccchi, K. Hristov, D. Klemm, C. Toldo, and O. Vaughan, Rotating black holes in 4d gauged supergravity, *J. High Energy Phys.* **01** (2014) 127.
- [116] D. Wu and P. Wu, Null hypersurface caustics for high-dimensional superentropic black holes, *Phys. Rev. D* **103**, 104020 (2021).

- [117] D. Wu, P. Wu, H. Yu, and S.-Q. Wu, Notes on the thermodynamics of superentropic AdS black holes, *Phys. Rev. D* **101**, 024057 (2020).
- [118] D. Wu, P. Wu, H. Yu, and S.-Q. Wu, Are ultraspinning Kerr-Sen-AdS₄ black holes always superentropic?, *Phys. Rev. D* **102**, 044007 (2020).
- [119] D. Wu, S.-Q. Wu, P. Wu, and H. Yu, Aspects of the dyonic Kerr-Sen-AdS₄ black hole and its ultraspinning version, *Phys. Rev. D* **103**, 044014 (2021).
- [120] D. Wu and S.-Q. Wu, Ultra-spinning Chow's black holes in six-dimensional gauged supergravity and their thermodynamical properties, *J. High Energy Phys.* **11** (2021) 031.
- [121] S.M. Noorbakhsh and M. Ghominejad, Ultra-spinning gauged supergravity black holes and their Kerr/CFT correspondence, *Phys. Rev. D* **95**, 046002 (2017).
- [122] S.M. Noorbakhsh and M.H. Vahidinia, Extremal vanishing horizon Kerr-AdS black holes at ultraspinning limit, *J. High Energy Phys.* **01** (2018) 042.
- [123] S.-Q. Wu and D. Wu, Thermodynamical hairs of the four-dimensional Taub-Newman-Unti-Tamburino spacetimes, *Phys. Rev. D* **100**, 101501 (2019).
- [124] D. Wu and S.-Q. Wu, Consistent mass formulas for the four-dimensional dyonic NUT-charged spacetimes, *Phys. Rev. D* **105**, 124013 (2022).
- [125] D. Wu and S.-Q. Wu, Consistent mass formulas for higher even-dimensional Taub-NUT spacetimes and their AdS counterparts, *Phys. Rev. D* **108**, 064034 (2023).
- [126] D. Wu and S.-Q. Wu, Revisiting mass formulas of the four-dimensional Reissner-Nordström-NUT-AdS solutions in a different metric form, *Phys. Lett. B* **846**, 138227 (2023).
- [127] S.-Q. Wu and D. Wu, Consistent mass formulas for higher even-dimensional Reissner-Nordström-NUT-AdS spacetimes, *Phys. Rev. D* **108**, 064035 (2023).
- [128] S.-Q. Wu and D. Wu, Is the type-D NUT C-metric really "missing" from the most general Plebański-Demiański solution?, [arXiv:2409.06733](https://arxiv.org/abs/2409.06733).